Journal of
Materials Chemistry

Cite this: *J. Mater. Chem.*, 2011, **21**, 3672

www.rsc.org/materials

PAPER

Magnetically assembled photonic crystal film for humidity sensing

Ruyang Xuan,[a] Qingsheng Wu,[a] Yadong Yin[b] and Jianping Ge*[ab]

Received 5th November 2010, Accepted 7th January 2011
DOI: 10.1039/c0jm03790g

A novel Fe_3O_4@SiO_2/PEG acrylate photonic crystal humidity sensor has been fabricated by combining magnetic assembly and photo-polymerization. The sensor self-displays brilliant colors as the humidity changes. By optimizing the cross-linking level and the thickness of the polymer film, the reflection wavelength can shift 160 nm in several minutes, while its intensity is readable by the naked eye. The tested sensors demonstrate good reversibility and durability in cycling experiments. Such photonic crystal sensors may have great potential as energy efficient devices, as no electric power is required for their operation.

Introduction

Humidity monitoring has attracted increasing attention in past decades due to its importance in agricultural production, weather forecasting, environmental control, food storage and many chemical processes. Great efforts have been made to manufacture different types of humidity sensors, which indicate humidities by detecting the changes in resistance,[1–6] capacitance,[7–9] surface acoustic wave (SAW),[10–12] diffraction[13–17] and reflection,[18,19] transmittance,[20] fluorescent emission,[21–23] deflection of a cantilever,[24] and the mass-related frequency of a quartz crystal resonator.[25,26] Today, the electrical based humidity sensor has been commercialized and widely applied. However, in many cases, low cost, convenient and visually readable colorimetric sensors, which require no specific apparatus for operation and cause no power consumption, are highly desired.

A responsive photonic crystal (RPC) offers a good solution to this challenge, because it is capable of changing its photonic band gap properties by external stimulus,[27–39] *e.g.* humidity fluctuations, and simultaneously diffracting brilliant colors under sunlight or indoor illumination. These RPC-based visual sensors operate through the changes in the lattice constant and/or refractive index contrast of the crystals, which are typically achieved by introducing a stimuli responsive polymer into the interstices of the colloidal packing. For instance, Tian *et al.* reported a hydrogel sensor by infiltrating the solution of acrylamide into a styrene/methyl methacrylate/acrylic acid copolymerized (p(St–MMA–AA)) colloidal crystal template and polymerizing the monomer.[14] Huang *et al.* fabricated a macroporous poly(ionic liquid) sensing film from a SiO_2 colloidal crystal template.[15] Although colorimetric detection of humidity has been realized, the widespread practical applications of these prior systems have not been demonstrated because they all heavily rely on colloidal crystal templates, whose large scale fabrication at low cost has remained a great challenge.

In this work, we report a process that allows the fast fabrication of a new RPC-based humidity sensing film, whose performance can be controlled by the cross-link level and the thickness of the polymer matrix. Unlike the traditional processes that involve colloidal assembly, monomer/oligomer infiltration, polymerization, and possibly an additional step of template removal, our process combines all of these steps into one, forming a 1D chain photonic structure and instantly producing large area, high quality, and monochromatic PC films on substrates of various compositions and arbitrary shapes, such as glass slides, silicon wafers, or plastic plates.[40] More specifically, this process starts with a thin film containing super-paramagnetic Fe_3O_4@SiO_2 colloids and a liquid precursor of poly(ethylene glycol) acrylates, and then produces humidity sensitive RPC film by creating photonic structures through instant magnetic assembly and then fixing the structures through photo-polymerization. The polymer matrix, which is composed of hygroscopic poly(ethylene glycol) methacrylate (PEGMA) and cross-linker poly(ethylene glycol) diacrylate (PEGDA), strongly absorbs water and therefore swells upon contact with humid air, leading to the increase of the lattice constant and color changes from blueish-green to red (Fig. 1). The colors are even brighter when the film is directly in contact with water. PEG based acrylates are known as optically transparent polymers with low toxicity compared to acrylamide based polymers, making them promising for many optical applications. The diffraction peak red-shifts *ca.* 220 nm when the humidity changes from 22% to 100%, meaning that the color change can cover the whole visible range if an appropriate starting lattice constant is designed. The responding sensitivity and speed can be optimized by tuning the cross-linking level and the thickness of the polymer matrix. Such a self-display sensor has intrinsic advantages for daily and

---

[a] *Department of Chemistry, Tongji University, Shanghai, 200092, China. E-mail: gejianping09@tongji.edu.cn; Tel: +86 21 65982653*
[b] *Department of Chemistry, University of California, Riverside, CA, 92521, USA*

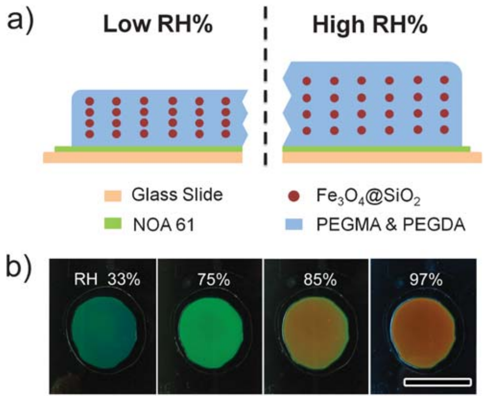

Fig. 1 (a) A schematic illustration of the structure of the humidity sensing film and the mechanism of color switching between low and high RH environments. (b) Digital photos of a typical film with a 50% cross-link level in different humidity environments, showing blueish-green, green, yellow and red, accordingly. The scale bar is 1 cm.

household usage, as the colors are visually accessible and reproducible. It also represents a unique humidity sensing system which can be conveniently made into large area colorimetric indicators that require no power for long-term operation.

Experimental section

Chemicals

Anhydrous iron(III) chloride ($FeCl_3$, 97%), diethylene glycol (DEG, 99%), poly(acrylic acid) (PAA, $M_w = 1800$), 2-hydroxyethyl methacrylate (HEMA, 99%), poly(ethylene glycol) methacrylate (PEGMA, $M_n = 360$), poly(ethylene glycol) diacrylate (PEGDA, $M_n = 700$), and 2,2-dimethoxy-2-phenylacetophenone (DMPA, 99%) were purchased from Sigma-Aldrich. Sodium hydroxide (NaOH, 99%), tetraethylorthosilicate (TEOS, 98%), and ammonium hydroxide solution (28%) were purchased from Sinopharm Chemical Reagent Co.

Fabrication of photonic crystal film

Super-paramagnetic Fe_3O_4 colloids were prepared using a high temperature hydrolysis reaction,[41] and then coated with a silica layer through a modified Stober process. Magnetic colloids and photo-initiator DMPA (5 wt%) were dispersed in the mixture of PEGDA and PEGMA with various volume ratios to form a brown homogeneous solution with a magnetite concentration of 8 mg mL^{-1}. In a typical process, a precuring mixture (25 μL) was sandwiched between a regular cover glass and a fluorinated glass slide, placed 1 cm above a rectangular NdFeB magnet (5 × 5 × 1 cm), and 5 cm beneath a strong UV light source (Spectroline SB-100P, 365 nm) for photo-polymerization. The curing time for PEGDA solution and a mixture of PEGDA and PEGMA are 1 min and 3 min, respectively. After curing, the solid film was easily separated from the hydrophobic glass and fixed onto the glass substrate using the commercial optical adhesive (Norland OA61). To obtain a reproducible optical response, the film was washed with water several times and dried in a 50 °C oven to remove the residue.

Characterization

A Hitachi S4800 scanning electron microscope (SEM) was used to investigate the morphology of the surface and cross-section of photonic crystal films. A Sony T7 digital camera was used to present the colors of the film. The photos were taken without flash light to minimize the inaccuracy caused by color treatment by the camera. The diffraction spectra were all measured by Ocean Optics USB-4000 UV-vis spectrometer coupled to a six-around-one reflection probe. All reflections were measured with incident and reflection angles of 0°, as shown in Fig. 2.

Reflection measurements

For the reflection measurement of the photonic crystal film under different humidities, several saturated salt solutions were used to create a stable environment with accurate humidity. The relative humidities (RH) of 11, 33, 54, 75, 85, 97% can be provided as saturated solutions of LiCl, $MgCl_2$, $Mg(NO_3)_2$, NaCl, KCl or K_2SO_4 stored in a closed chamber. Typically, a petri dish 90 mm in diameter and 15 mm in height is filled with 50 mL saturated solution, which creates a humidity chamber of 45 cm^3 above the solution. The photonic crystal film is placed inside the chamber for 2 h, and the corresponding reflection spectra are recorded by a UV-vis spectrometer.

In order to investigate the contribution of the photonic crystal film to the humidity fluctuation and the reproducibility of the reflection signals, a petri dish 50 mm in diameter and 10 mm in height was used to fabricate a small closed chamber, in which the humidity can be tuned between 22% and 100% by introducing dry or wet air. As shown in Fig. 2, the wet air is produced by bubbling the water at 40 °C, and the dry air is provided by the gas cylinder without further treatment. A commercial hygrometer is enclosed to indicate the real-time humidity of the chamber. The air flows out from the hole in the cover of the petri dish, where the probe of the spectrometer is placed perpendicularly to the photonic crystal film. As the humidity changes, the reflections are recorded every one or two minutes, which monitors the variation of the crystal structure in real-time.

Results and discussion

The photonic humidity sensor is prepared through the fast magnetic self-assembly of Fe_3O_4@SiO_2 colloids, followed by an instant UV curing process to fix the photonic structures inside a cross-linked PEG acrylate matrix. The cross-linking level of the

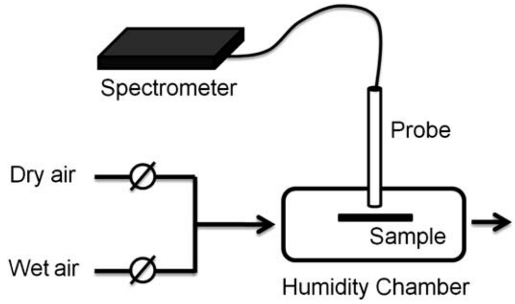

Fig. 2 The experimental setup for the reflection measurement of the photonic crystal film in an environment with adjustable humidity.

polymer matrix is controlled by mixing PEGMA and PEGDA oligomers in various ratios. Unlike the porous PEG acrylate hydrogel polymerized in solution,[42,43] the polymer films synthesized in the absence of water have a relatively dense network, which means that the position of the colloidal particles can be fixed in a broad range of cross-link levels. Scanning electron microscope (SEM) images (Fig. 3) obtained from the cross-section of the film show that the colloids form chain-like structures with uniform interparticle spacings of *ca.* 190 nm along the external magnetic field, which is responsible for the strong diffraction of visible light. The volume fraction of colloidal particles in this photonic crystal film (*ca.* 0.1%) is much lower than that of 3D colloidal crystals (74%). The neighboring particle chains have an interspacing of 2–3 μm due to magnetic repulsion, therefore only several isolated lines can be shown in a SEM image. The large contrast of refractive indices between particle and polymer as well as the staggered arrangement of chains at different depths to the film surface are responsible for the visible diffraction even in such diluted conditions. Transmission electron microscope (TEM) results (Fig. 4) also demonstrate an average magnetic core diameter of 97 nm and a shell thickness of about 34.5 nm, giving a reasonable 24 nm surface separation as Fe_3O_4@SiO_2 colloids disperse in PEG acrylate. With less cross-linker added, the polymer matrix turns softer and more flexible; which can be proved by the fact that the holes produced by dropping colloids become much easier to deform or collapse under illumination by the electron beam.

For the purpose of humidity measurement, sensitivity is one of the most important parameters to evaluate the sensors. In the case of self-display photonic crystal sensors, sensitivity can be simply characterized by the shift of the diffraction peak, where a larger diffraction wavelength change ($\Delta\lambda$) means a sharper color change and clearer identification of different humidities. As shown in Fig. 5, a series of experiments are thereby designed to investigate the relationship between $\Delta\lambda$ and the cross-linking level (CL). Highly cross-linked Fe_3O_4@SiO_2/PEGDA film (100% CL) was firstly found to have a moistening effect. With the humidity increasing from 11% to 97%, a total red-shift of 133 nm in diffraction can be achieved, since the lattice constant increases as the polymer swells in humid air, seen in Table 1. According to our previous research,[40] the influence of the change in the refractive index is limited, and the variation of the lattice constant is a dominant reason for the color changes. As the humidity reaches 100%, a maximum $\Delta\lambda$ of 159 nm can be observed, which is comparable to most of the best literature values. In order to improve the sensitivity, namely to increase $\Delta\lambda$, it is reasonable to synthesize a more flexible polymer network for easier deformation.

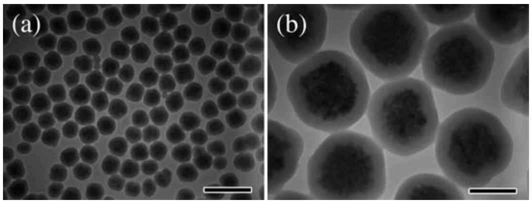

Fig. 4 TEM images of the Fe_3O_4@SiO_2 core/shell colloidal particles used in the fabrication of photonic crystal humidity sensor. The scale bars in (a) and (b) are 400 and 100 nm, respectively.

It is known that a highly cross-linked polymer could be very rigid and glassy, while a polymer with an intermediate CL level becomes more elastomeric. On the basis of this understanding, we constructed a polymer network with a lower CL degree by copolymerizing PEGDA with PEGMA, which is a hydrophilic oligomer with a single acrylate group. A monomer with an analogous molecular structure is selected here to guarantee good dispersibility of the magnetic colloids, transparent optical properties, and fast copolymerization using the current synthetic system. With a decrease of cross-linking from 100% to 20%, $\Delta\lambda$ at a humidity of 97% and 100% increased to 175 and 222 nm, respectively, which proves that the sensitivity of the sensor can be greatly enhanced by tuning the flexibility of the polymer matrix. As the cross-link further decreases to a critically low level (5%), the wavelength change may slightly fall back (several nm) due to the decrease in the elasticity of the polymer matrix. It should be

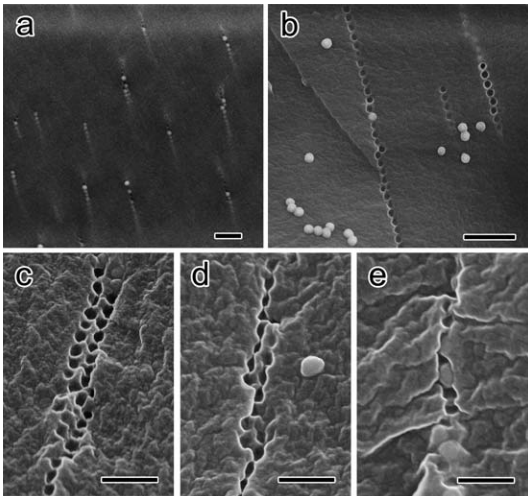

Fig. 3 SEM images of the cross sections of Fe_3O_4@SiO_2/PEG acrylate photonic crystal films with cross-linking levels of (a, b) 100%, (c) 50%, (d) 20%, and (e) 5%. The scale bars in (a) and (b) are 1 μm, and those in (c)–(e) are 500 nm.

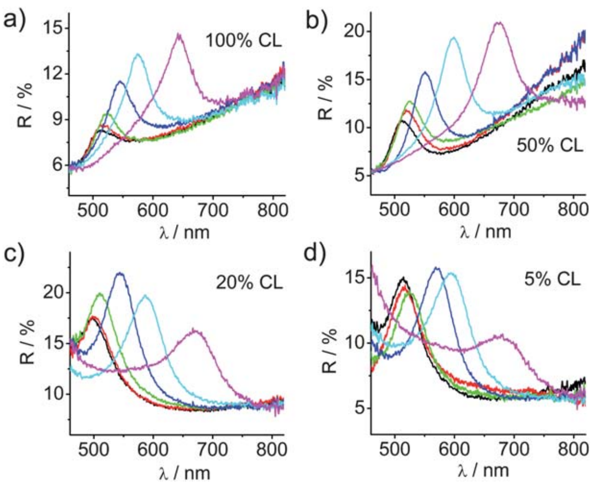

Fig. 5 Balanced diffractions of Fe_3O_4@SiO_2/PEG acrylate film with a cross-link level of (a) 100%, (b) 50%, (c) 20% and (d) 5% in a closed system. Diffraction peaks gradually red-shift as the humidity increases from 11, 33, 54, 75, 85, to 97%.

Table 1 The diffraction wavelength change ($\Delta\lambda$/nm) of PC films with different CL levels in a closed system with various humidities.

CL%	RH% 11	33	54	75	85	97	100[a]
100	0	5.8	13.4	36.1	64.0	133.2	159.0
50	0	7.5	13.2	38.3	85.5	162.2	175.0
20	0	2.3	13.2	46.2	88.8	175.2	222.0
5	0	2.9	12.5	59.1	85.2	171.7	231.0

[a] $\Delta\lambda$ at 100% humidity was calculated from Fig. 6a.

noted that $\Delta\lambda$ at low humidity scale (<50%) barely improves with a decrease in the CL, probably because the small deformation of photonic crystal film within this humidity range can hardly be affected by the change in the flexibility of the polymer network.

In addition to sensitivity, response speed can be improved by tuning the CL level as well. For investigation of response time, a small closed chamber was constructed in a petri dish, in which the humidity can be tuned by introducing dry or wet air. Fig. 6a compares the time dependence of the change in the diffraction wavelength for PC films with different CL levels in a single cycle as humidity increases to 100% and falls back to 22%. Diffraction patterns were recorded every one or two minutes to track the peak shift. Defining response time as that required to reach 90% variation of balanced $\Delta\lambda$, it is calculated to be 58, 52, 50 and 70 min during the humidifying stage as the CL level decreases from 100% to 5%, and it is determined to be 44, 26, 29 and 40 min for the drying stage, respectively. Fig. 6c shows that the sensing film with 20% CL has the fastest response when the polymer swells, and that with 50% CL performs best as the polymer shrinks.

The response speed can be further improved by decreasing the thickness of the polymer film, since the diffraction shift or color change is actually controlled by the absorption and diffusion of water molecules inside the polymer. For typical sensing films with a CL of 50%, with the thickness decreasing from 240 to 30 µm, the response time of swelling and shrinking decreases tremendously from 52 and 26 min to 9 and 3 min, respectively. (Fig. 6d) When water molecules in humid air are absorbed in the surface layer of the PC film, they diffuse down to the deeper layer. Stable diffraction can be obtained only after the whole polymer is swelled, which leads to a slow response for thicker films. Appropriately, decreasing the thickness will not affect the sensitivity and visual readability of the sensors. Although further decreasing the thickness below 30 µm may bring an even faster response in spectrometer measurement, the optical signals are not easy to recognize by the naked eye. There are few reports focused on the dynamic response of photonic crystal humidity sensors. Most works report the diffraction shift in the equilibrium state, which takes a long time to guarantee the balanced deformation. Tian *et al.* prepared a polyacrylamide (PAAm) filled P(St–MMA–AA) PC hydrogel, which shifted its stopband (230 nm) in 1.5 h.[14] The porous photonic structure has a relatively fast response. Barry *et al.* fabricated a PAAm inverse-opal hydrogel, which shifted the stopband (30 nm) within 20 s.[17] For a nonporous photonic structure reported in this manuscript, the stopband shifting across a broad range of 160 nm within 10 min is acceptably fast for daily usage. Compared with commercial electric sensors, the response time of RPC-based sensors still has much room for improvement, but there is no doubt that they will find practical applications in daily household usage where humidity may not change swiftly.

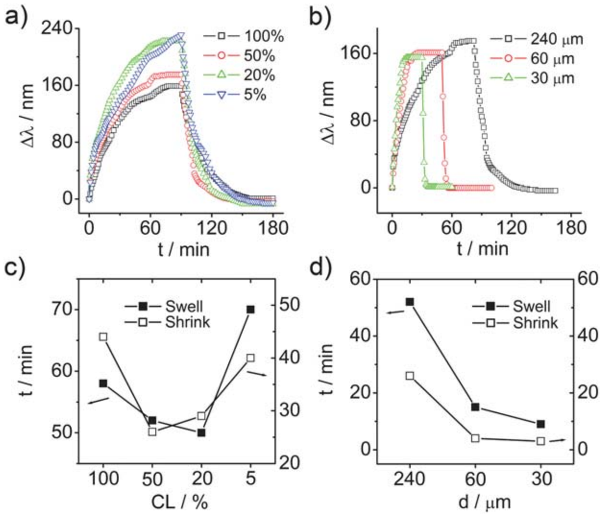

Fig. 6 The time dependence of the change in the diffraction wavelength ($\Delta\lambda$) for PC films with different (a) CL levels and (b) thicknesses in a single cycle as humidity increases to 100% and recovers to 22%. The response time for PC sensors with various (c) CL levels and (d) thicknesses.

The samples presented good reversibility and durability during the cycling experiments. The measurement in Fig. 5 has been repeated several times, and the results are very close to each other. Fig. 7 shows a reversible change in the diffraction wavelength in 5 continuous cycles as the humidity switches between 100% and 22%, which demonstrates that the sensor can be used many times within the major humidity range.

The properties of the polymer matrix are found to be critical to the performance of the polymer composite photonic structures. Firstly, for the current system, the monomer should be hydrophilic for good dispersion of magnetic colloids and a fast response to humid air. For comparison, methyl methacrylate (MMA) and 2-hydroxyethyl methacrylate (HEMA) were copolymerized with PEGDA to fabricate a soft polymer film with a similar CL level to the PEGMA–PEGDA film. However, such a film responds much more slowly due to the lower hydrophilicity of MMA or HEMA compared with PEGMA. Secondly, the polymer matrix should be optically transparent and quickly polymerized, in case the particles separate from the solution before the photonic structure is stabilized. Thirdly, the polymer

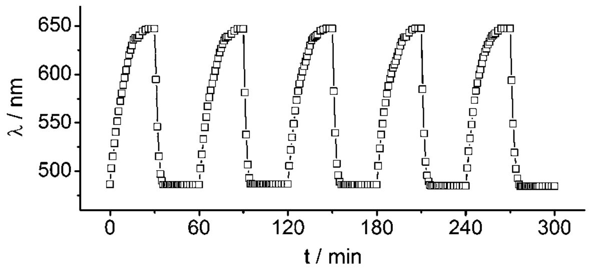

Fig. 7 The reversible change in the diffraction wavelength for PC films with a cross-link level of 50% and thickness of 60 µm in 5 continuous cycles as humidity switches between 100% and 22%.

matrix should have an appropriate cross-link level and thickness for optimal performance. With a decrease in the CL level, the polymer matrix becomes more flexible and easier to deform, so that both the sensitivity and the response rate improve. Further decreasing of the CL level after reaching a critical value will cause the polymer to become less elastic, leading to reduced sensitivity and response rate. This is because the film fixed on the substrate mainly swells along the vertical direction, which is actually enhanced by the limitation of horizontal swelling and requires the polymer matrix to be firm and elastic. With the cross-linking level decreased to a critically low level, the influence of elasticity loss becomes dominant, so that the increase in $\Delta\lambda$ was retarded or even reversed in some cases. Although $\Delta\lambda$ reaches a maximal value for a 5% CL film, the durability of such a film can be a big concern, since the film will infinitely swell and break in high humidity environments. Our systematic studies show that $Fe_3O_4@SiO_2$/PEG acrylate film with a CL of around 50% and a thickness of about 60 μm has the best overall performance.

Conclusion

In summary, we have demonstrated a convenient procedure for the fabrication of a photonic crystal based humidity sensor by combining rapid magnetic assembly and photo-polymerization. The as-prepared composite film is sensitive to humidity, since it will swell in humid air and shrink in dry air, which leads to visual color changes due to an increase or decrease in the lattice constant. Through investigation of the sensitivity and response rate for various samples, the cross-linking level and film thickness are found to be effective parameters to optimize the performance of these polymeric photonic structures. A large shift of 160 nm in the diffraction wavelength can be realized in several minutes, which is fast for visual photonic sensors. The tested sensors demonstrate good reversibility and durability in cycling experiments. Considering its low cost production and zero power consumption, we believe that the self-displaying and environmentally friendly PC-based sensors should be able to find broader applications after appropriate modification.

Acknowledgements

Dr Ge thanks the support from National Science Foundation of China (NSFC 21001083), Shanghai Pujiang Program (10PJ1409800), and Tongji University start-up fund. Dr Yin thanks the US National Science Foundation for financial support. Acknowledgement is also made to Dr Sun in Beijing University of Chemical Technology and Mr. Hu in Experimental Chemistry Center in Tongji University for TEM and SEM analysis.

Reference

1 Q. Kuang, C. S. Lao, Z. L. Wang, Z. X. Xie and L. S. Zheng, *J. Am. Chem. Soc.*, 2007, **129**, 6070–6071.
2 X. H. Zhang, S. A. McGill and P. Xiong, *J. Am. Chem. Soc.*, 2007, **129**, 14470–14474.
3 Z. Y. Li, H. N. Zhang, W. Zheng, W. Wang, H. M. Huang, C. Wang, A. G. MacDiarmid and Y. Wei, *J. Am. Chem. Soc.*, 2008, **130**, 5036–5037.
4 X. L. Hu, J. M. Gong, L. Z. Zhang and J. C. Yu, *Adv. Mater.*, 2008, **20**, 4845–4850.
5 Z. H. Yang, Z. Cao, H. Sun and Y. Li, *Adv. Mater.*, 2008, **20**, 2201–2205.
6 Y. Zhou, J. D. Grunwaldt, F. Krumeich, K. B. Zheng, G. R. Chen, J. Stotzel, R. Frahm and G. R. Patzke, *Small*, 2010, **6**, 1173–1179.
7 Y. Wang, S. Park, J. T. W. Yeow, A. Langner and F. Muller, *Sens. Actuators, B*, 2010, **149**, 136–142.
8 C. L. Dai, *Sens. Actuators, B*, 2007, **122**, 375–380.
9 L. M. Zambov, C. Popov, N. Abedinov, M. F. Plass, W. Kulisch, T. Gotszalk, P. Grabiec, I. W. Rangelow and R. Kassing, *Adv. Mater.*, 2000, **12**, 656–660.
10 X. W. Zhan, M. J. Yang, Z. Q. Lei, Y. Li, Y. Q. Liu, G. Yu and D. B. Zhu, *Adv. Mater.*, 2000, **12**, 51–53.
11 X. T. Qiu, R. Tang, J. Zhu, J. Oiler, C. J. Yu, Z. Y. Wang and H. Y. Yu, *Sens. Actuators, B*, 2010, **147**, 381–384.
12 H. S. Hong and G. S. Chung, *Sens. Actuators, B*, 2010, **148**, 347–352.
13 M. Takahashi, M. Inoue, R. Ihara, T. Yoko, T. Nemoto, S. Isoda, L. Malfatti, S. Costacurta and P. Innocenzi, *Adv. Mater.*, 2010, **22**, 3303–3306.
14 E. T. Tian, J. X. Wang, Y. M. Zheng, Y. L. Song, L. Jiang and D. B. Zhu, *J. Mater. Chem.*, 2008, **18**, 1116–1122.
15 J. Huang, C. A. Tao, Q. An, C. X. Lin, X. S. Li, D. Xu, Y. G. Wu, X. G. Li, D. Z. Shen and G. T. Li, *Chem. Commun.*, 2010, **46**, 4103–4105.
16 M. Karaman, S. E. Kooi and K. K. Gleason, *Chem. Mater.*, 2008, **20**, 2262–2267.
17 R. A. Barry and P. Wiltzius, *Langmuir*, 2006, **22**, 1369–1374.
18 J. W. Grate, L. K. Moore, D. E. Janzen, D. J. Veltkamp, S. Kaganove, S. M. Drew and K. R. Mann, *Chem. Mater.*, 2002, **14**, 1058–1066.
19 J. Estella, P. de Vicente, J. C. Echeverria and J. J. Garrido, *Sens. Actuators, B*, 2010, **149**, 122–128.
20 F. X. Gu, L. Zhang, X. F. Yin and L. M. Tong, *Nano Lett.*, 2008, **8**, 2757–2761.
21 J. Xu, W. X. Zhang, Z. H. Yang, S. X. Ding, C. Y. Zeng, L. L. Chen, Q. Wang and S. H. Yang, *Adv. Funct. Mater.*, 2009, **19**, 1759–1766.
22 J. Kunzelman, B. R. Crenshaw and C. Weder, *J. Mater. Chem.*, 2007, **17**, 2989–2991.
23 F. Galindo, J. C. Lima, S. V. Luis, M. J. Melo, A. J. Parola and F. Pina, *J. Mater. Chem.*, 2005, **15**, 2840–2847.
24 S. Singamaneni, M. E. McConney, M. C. LeMieux, H. Jiang, J. O. Enlow, T. J. Bunning, R. R. Naik and V. V. Tsukruk, *Adv. Mater.*, 2007, **19**, 4248–4255.
25 A. Erol, S. Okur, B. Comba, O. Mermer and M. C. Arikan, *Sens. Actuators, B*, 2010, **145**, 174–180.
26 S. Korposh, R. Selyanchyn and S. W. Lee, *Sens. Actuators, B*, 2010, **147**, 599–606.
27 J. M. Weissman, H. B. Sunkara, A. S. Tse and S. A. Asher, *Science*, 1996, **274**, 959–960.
28 J. H. Holtz and S. A. Asher, *Nature*, 1997, **389**, 829–832.
29 A. C. Arsenault, T. J. Clark, G. Von Freymann, L. Cademartiri, R. Sapienza, J. Bertolotti, E. Vekris, S. Wong, V. Kitaev, I. Manners, R. Z. Wang, S. John, D. Wiersma and G. A. Ozin, *Nat. Mater.*, 2006, **5**, 179–184.
30 A. C. Arsenault, D. P. Puzzo, I. Manners and G. A. Ozin, *Nat. Photonics*, 2007, **1**, 468–472.
31 Z. Z. Gu, T. Iyoda, A. Fujishima and O. Sato, *Adv. Mater.*, 2001, **13**, 1295–1298.
32 Y.-J. Zhao, X.-W. Zhao, J. Hu, J. Li, W.-Y. Xu and Z.-Z. Gu, *Angew. Chem., Int. Ed.*, 2009, **48**, 7350–7352, S7350/7351-S7350/7355.
33 S. H. Foulger, P. Jiang, A. Lattam, D. W. Smith, J. Ballato, D. E. Dausch, S. Grego and B. R. Stoner, *Adv. Mater.*, 2003, **15**, 685–689.
34 Y. Kang, J. J. Walish, T. Gorishnyy and E. L. Thomas, *Nat. Mater.*, 2007, **6**, 957–960.
35 H. Fudouzi and Y. N. Xia, *Adv. Mater.*, 2003, **15**, 892–896.
36 C. I. Aguirre, E. Reguera and A. Stein, *Adv. Funct. Mater.*, 2010, **20**, 2565–2578.
37 V. Rastogi, S. Melle, O. G. Calderon, A. A. Garcia, M. Marquez and O. D. Velev, *Adv. Mater.*, 2008, **20**, 4263–4268.
38 P. D. Garcia, R. Sapienza and C. Lopez, *Adv. Mater.*, 2010, **22**, 12–19.
39 X. L. Xu, G. Friedman, K. D. Humfeld, S. A. Majetich and S. A. Asher, *Adv. Mater.*, 2001, **13**, 1681–1684.
40 J. Ge, J. Goebl, L. He, Z. Lu and Y. Yin, *Adv. Mater.*, 2009, **21**, 4259–4264.
41 J. Ge, Y. Hu, M. Biasini, W. P. Beyermann and Y. Yin, *Angew. Chem., Int. Ed.*, 2007, **46**, 4342–4345.
42 G. X. Tan, Y. J. Wang, J. Li and S. J. Zhang, *Polym. Bull.*, 2008, **61**, 91–98.
43 H. Q. Lin, T. Kai, B. D. Freeman, S. Kalakkunnath and D. S. Kalika, *Macromolecules*, 2005, **38**, 8381–8393.